論文 / 著書情報
Article / Book Information

Title	Properties of Viscoelastic Damper under Wind Load and Analytical Methods Considering Heat Conduction & Transfer
Authors	Daiki Sato, Kazuhiko Kasai, Tetsuro Tamura
Citation	Properties of 12th International Conference on Wind Engineering ICWE12, , , pp. 1263-1270
Pub. date	2007, 7

Properties of Viscoelastic Damper under Wind Load and Analytical Methods Considering Heat Conduction & Transfer

Daiki Sato [a], Kazuhiko Kasai [a], Tetsuro Tamura [b]

[a] *Tokyo Institute of Technology, G5-14, 4259, Nagatuta, Midori-ku Yokohama, Japan*
[b] *Tokyo Institute of Technology, G5-7, 4259, Nagatuta, Midori-ku Yokohama, Japan*

ABSTRACT: Viscoelastic damper dissipates energy through shear deformation of the viscoelastic material, and this causes temperature rise and softening of the material. Under long duration load, therefore significant heat conduction and transfer can occur and control the temperature-rise effects. These and frequency sensitivities are considered in the two analysis methods proposed: The first method combines three-dimensional heat transfer analysis and static analysis using a common finite element model of the damper, and it estimates damper dynamic properties under long duration load. The second combines one-dimensional heat transfer analysis and viscoelastic constitutive rule using fractional time-derivatives of stress and strain, and it calculates step-by-step the force-deformation time histories of the damper. In addition, a simplified evaluation method using sinusoidal-wave is proposed in this study, and the results obtained by this method show excellent accuracy the damper properties under long random loading.

KEYWORDS: Viscoelastic Damper, Fractional Derivative, Duration,
Heat Conduction, Heat Transfer, Finite Element Analysis.

1 INTRODUCTION

It has been recognized that viscoelastic (VE) dampers have significant advantage over other types of dampers in controlling responses of buildings against not only wind but also earthquake excitation. VE damper dissipates energy through shear deformation of the VE material, and making temperature rise and softening the material. Under long duration load, therefore, significant heat conduction and transfer can occur and control the temperature-rise effect.

Kasai et al [1], [2] proposed the nonlinear model of VE damper based on the fractional time-derivative with focus on the effect of temperature-rise. This model is called "Short duration model" in this study. However, this model dose not consider the heat conduction and heat transfer, which are still significant even in cases of short duration loading such as earthquake.

In case of long duration loading such as wind force, heat conduction and heat transfer effects must be considered. These effects and frequency sensitivities are considered in two analysis methods proposed in this study. The first method, which is called "3D-FEM method", combines three-dimensional heat transfer analysis and static analysis using a common finite element model of the damper, and estimates damper dynamic properties under long duration load. The second method, which is called "Long duration model", combines one-dimensional heat transfer analysis and viscoelastic constitutive rule using fractional time-derivatives of stress and strain, and it calculates step-by-step the force-deformation time histories of the damper. The accuracies of both analysis methods are demonstrated by comparing with the results of experiments applying cyclic loading of long duration.

Some cases of the long duration random loading analysis using the long duration model are carried out. In addition, the simplified evaluation method using sinusoidal-wave, without the random time history data, is proposed in this study.

2 LONG DURATION LOADING TEST

2.1 *Test Specimen Description and Test Setup*

Figure 1 shows the test specimen of VE damper. A long duration loading test of individual VE damper has been carried out to investigate characteristic of VE damper under long duration loading and to validate the proposed analytical methods. The damper is made from acrylic polymer VE material produced by 3M Corp., with brand name ISD 111. The two VE material laminations are bonded between outer steel plate and inner steel plate. The wide of VE lamination B = 37.6 mm, the length L = 50.8mm and the thickness of one VE lamination d_v = 13.3 mm. The total area of two VE material laminations area A_v = 3,817 mm^2. The thickness of one steel plate d_s = 4.8 mm.

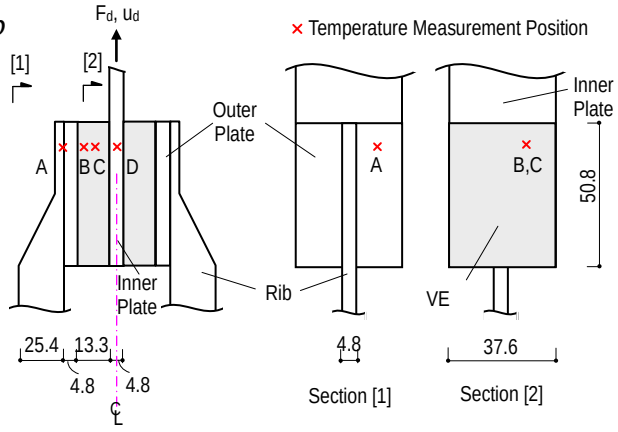

Figure 1. Test specimen & temperature measurement position. (unit: mm)

The sinusoidal displacement having peak amplitude $u_{d,max}$ = 6.6 mm (50% shear strain) and 3.0 seconds period is applied to the inner plate. The duration of sinusoidal wave is 3,000 seconds. After the excitation, decrease of damper temperature is monitored up to 5,000 seconds. Ambient temperature is maintained at 24 ^{o}C for 5,000 seconds.

As shown in Figure 1, the temperature of VE damper is measured at the four positions; (A) air side of outer steel plate, (B) 1/4 thickness of the VE lamination, (C) 1/2 thickness point of the VE lamination, and (D) center of inner steel plate.

2.2 *Long Duration Loading Test Results*

Figure 2 shows the time history of temperature at the each measurement position (See Figure 1) with the experimental results. As can be seen from Figure 2, it is recognized that the change of temperature is different depending upon the temperature measurement position. In addition, Figure 2 shows that temperature rise becomes sluggish and temperature is constant at each measurement point after 1,000 seconds. In case of under the long duration loading such as in this study, because of effect of the heat conduction & transfer to the steel plates, temperature of VE damper attains the steady state at a certain time, and temperature does not continue to rise even if the VE damper is still vibrating. After 3,000 seconds when the vibration finished, temperature of each point rapidly decreases to 24 ^{o}C because the internal heat generation inside the VE materials has stopped.

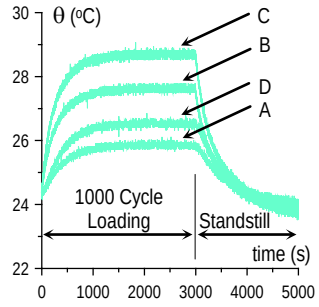

Figure 2. Temperature time history

Figure 3 shows the damper force F_d –deformation u_d relation during only 1st, 100th and 1,000th cycle. Figure 4 shows the change of the damper storage stiffness K'_d and loss stiffness K''_d [2] which are obtained from damper loop and calculated every 20 cycles.

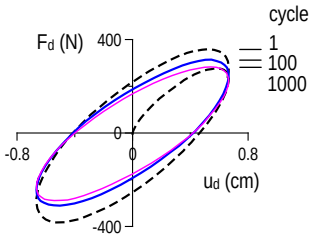

Figure 3. Force – deformation

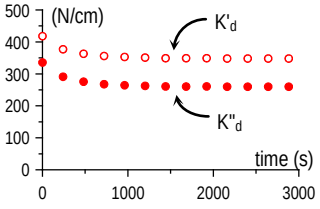

Figure 4. K'_d and K''_d

As Figure 4 indicates, K'_d and K''_d decrease immediately after loading. However, since temperature becomes steady state due to effect of the heat conduction & transfer as shown in Figure 2, K'_d and K''_d become constant too. Thus, this is an advantage of VE damper under the long duration loading, such as wind force.

3 3D-FEM ANALYSIS

3.1 *Algorithm of 3D-FEM Analysis*

As stated above, it is essential to consider the heat conduction & transfer to simulate exactly the properties of VE damper under the long duration loading. The two proposed methods in this chapter carry out alternately the static analysis and the unsteady or steady heat transfer analysis without dynamic analysis. So, the variation of temperature and stiffness of VE damper having the temperature dependency is simulated.

G'_j and η_j, which are the storage shear modulus and the loss factor of the viscoelastic material at the element j, are expressed by Eq. (1) [1], [2].

$$G'_j = G\frac{1+a_j b_j \omega^{2\alpha} + (a_j + b_j)\omega^{\alpha}\cos(\alpha\pi/2)}{1+a_j^2\omega^{2\alpha} + 2a_j\omega^{\alpha}\cos(\alpha\pi/2)}, \quad \eta_j = \frac{(-a_j + b_j)\omega^{\alpha}\sin(\alpha\pi/2)}{1+a_j b_j \omega^{2\alpha} + (a_j + b_j)\omega^{\alpha}\cos(\alpha\pi/2)} \tag{1a,b}$$

where, α = order of the fractional derivative; a_j, b_j and G = parameter of the fractional derivative. a_j and b_j are depended on temperature θ_j, and these are expressed as follows;

$$a_j = a_{ref}\lambda_j^{\alpha}, \quad b_j = b_{ref}\lambda_j^{\alpha}, \quad \lambda_j = \exp\left[-p_1(\theta_j - \theta_{ref})/(p_2 + \theta_j - \theta_{ref})\right] \tag{2a-c}$$

here, λ_j is called "shift factor", θ_{ref} = reference temperature; a_{ref}, b_{ref} = value of a, b at θ_{ref} respectively. The parameters of the fractional derivative for ISD 111 are; G = 6.516 N/cm^2, α = 0.609, a_{ref} = 0.015, b_{ref} = 21.157, θ_{ref} = 0.2°C, p_1 = 19.5 and p_2 = 80.2.

The storage modulus for axial direction E'_j is expressed, by using Poisson's ration ν, in Eq. (3).

$$E'_j = 2G'_j(1+\nu) \tag{3}$$

The algorithm of the 3D-FEM analysis is shown as follows:

Firstly, frequency ω, maximum damper deformation (amplitude) $u_{d,max}$, and initial temperature at element j θ_j are set. Then, G'_j, E'_j, η_j are calculated by using Eq. (1) ~ (3)

The static analysis that damper deformation is $u_{d,max}$ is carried out. The reaction force of damper F'_d is obtained. By multiplying $2\pi\eta_j$ by the strain energy of the element j obtained from the static analysis results, the dissipation energy per 1 cycle $W_{d,j}$ is obtained (Eq. (4))

$$W_{d,j} = \pi\eta_j V_j\left\{\sum_{k=1}^{3} E'_j\varepsilon_{kk,j}^2 + G'_j\left(\gamma_{12,j}^2 + \gamma_{23,j}^2 + \gamma_{31,j}^2\right)\right\} \tag{4}$$

where, V_j = volume of element j, $\varepsilon_{mn,j}$ and $\gamma_{mn,j}$ = strain at center of the element. Then, the damper storage stiffness K'_d and loss stiffness K''_d are calculated by Eq. (5)

$$K'_d = F'_d / u_{d,\max}, \quad K''_d = \left(\sum_j W_{d,j}\right) / (\pi u_{d,\max}^2) \tag{5a,b}$$

The heat generated per unit volume and unit time $\dot{Q}_j$ is expressed by Eq. (6).

$$\dot{Q}_j = W_{d,j} / (V_j T) \tag{6}$$

where, T = period of 1 cycle.

After damper deformation returns become zero, the unsteady-state heat transfer analysis using $\dot{Q}_j$ is carried out for T seconds. By using the temperature of each element θ_j obtained form the unsteady state heat transfer analysis result and Eq. (1) ~ (3), G'_j, E'_j, η_j are updated. For next cycle, the static analysis is carried out again. The above process is repeated.

The above method using the unsteady-state heat transfer analysis can be simulated the characteristic change such as stiffness and/or temperature of VE damper, but the calculation time is long. The calculation time becomes substantially short by replacing the unsteady-state heat transfer analysis with the steady-state heat transfer analysis.

3.2 *3D-FEM Model*

The 3D-FEM model is shown in Figure 5. Because this model is symmetric with respect to the center of inner plate, 3D-FEM is carried out by using half of this model. 3D coupled temperature-displacement solid elements (ABAQUS Ver. 6.4) are utilized in this model. The width of VE lamination B is divided into 18 elements, the length L is divided into 18 elements, the thickness d_v is divided into 12 elements, and 8,260 elements are used for this damper model.

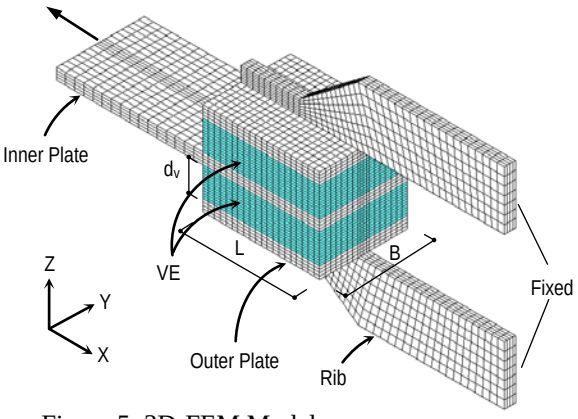

Figure 5. 3D-FEM Model

The inner palate is given the controlled displacement $u_{d,max}$ along X-direction. The end of rib is fixed, and the reaction force of VE damper F'_d can be obtained. The inner plate can not move in Y- and Z-direction. The symmetric surface, the center of inner plate, is set as insulation boundary condition. The ambient temperature θ_c = 24°C, same as the test condition.

Table 1. Parameter of 3D-FEM model

	Steel	VE
κ (N/s/°C)	43.128	0.188
s (N·cm/kg/°C)	46.63×10^{3}	19.40×10^{4}
ρ (kg/cm^3)	7.80×10^{-3}	1.0×10^{-3}
α_c (N/s/cm/°C)	0.25	0.25

1 N/s/cm/°C = 100 W/m^2/°C

The parameters which are used by 3D-FEM model are shown in Table 1. Where, κ = thermal conductivity, s = specific heat, ρ = density, α_c = heat-transfer coefficient. α_c is obtained by using a trail-and-error method referring to Reference [3], and we decided to use α_c = 0.25 N/s/cm//°C in this study. This value means that this situation is between "free convection" and "forced convection" [3]. Poisson ratio of VE material is 0.47, steel is 0.3, and Young's modulus of steel is 2.05 x 10^7 N/cm^2.

3.3 *Comparison between Test and 3D-FEM Analysis Results*

Figure 6 shows the result of the temperature and Figure 7 shows K'_d and K''_d, which are obtained from the test and the two types of 3D-FEM analysis which are unsteady-state and steady-state analysis as stated above. As shown in Figure 6 and 7, the analytical results are in good agreements with the test results.

The temperature distributions calculated by 3D-FEM analysis are shown in Figure 8. The distribution along Z-direction has different temperature on each point, however the temperature on X-Y section has uniform distribution except of the extreme portion of the surface.

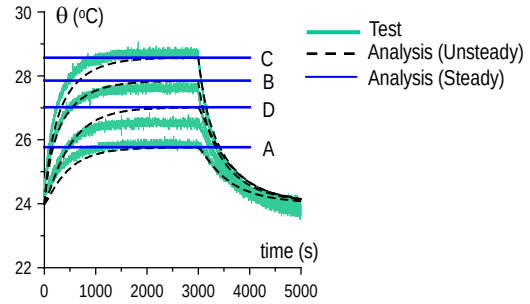

Figure 6. Comparison of temperature with test and 3D-FEM

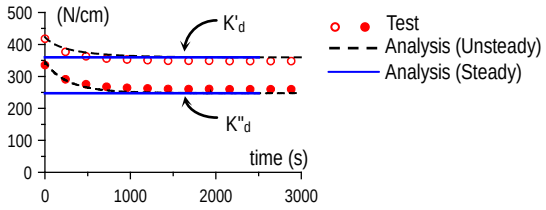

Figure 7. Comparison of K'_d , K''_d with test and 3D-FEM

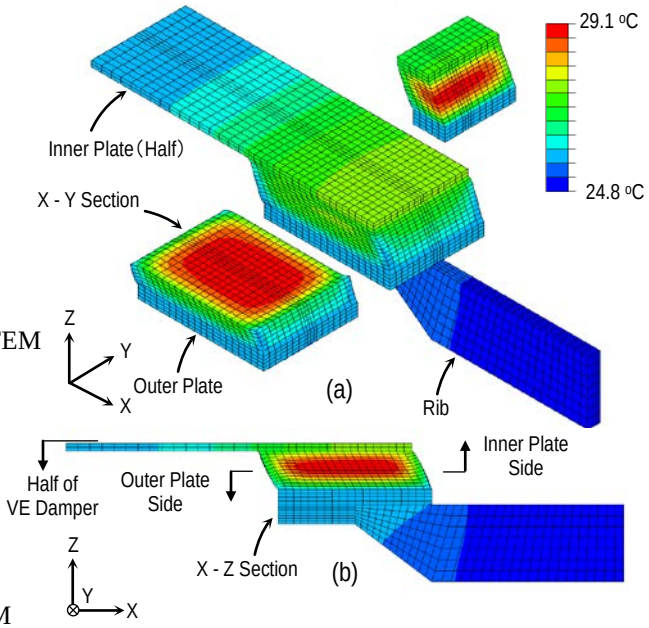

Figure 8. Temperature distribution at 3,000 sec

4 TIME HISTORY ANALYSIS METHOD (LONG DURATION MODEL)

4.1 *Algorism of Long Duration Model*

The nonlinear model of VE damper was proposed earlier by Kasai et al. [1], [2], and it is called "Short duration model". However, this model does not consider the heat conduction and heat transfer, which are still reasonable in case of short duration load like an earthquake.

From the results of 3D-FEM analysis in Figure 8, it is recognized that the temperature distribution inside the VE damper can be express by using one–dimensional (1D) heat problem. In this chapter, the time history analysis method combining one-dimensional heat transfer analysis is proposed, and it is called "long duration model". It combines 1D heat transfer analysis and viscoelastic constitutive rule using fractional time-derivatives of stress and strain, and it calculates step-by-step the force-deformation time histories of the damper.

Figure 9 shows the example that VE damper thickness is divided into 10 elements (m = 10; m = total element number of the long duration model). Where j is node number, and the nodes j_1 to j_2 are VE material, other nodes are steel part, and d_j is length of j element.

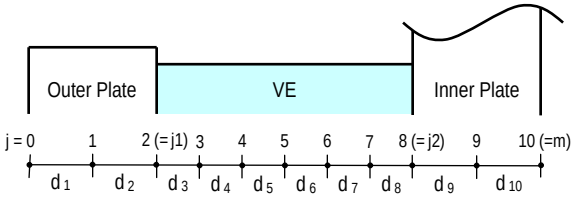

Figure 9. Example of element division for damper

When n^{th} step damper deformation $u_d^{(n)}$ is known, the compatibility equation between the damper deformation $u_d^{(n)}$ and shear strain at element j $\gamma_j^{(n)}$ can be expressed by Eq. (7).

$$u_d^{(n)} = \frac{1}{2}\sum_{j=j_1}^{j_2} \zeta_j \gamma_j^{(n)} \tag{7}$$

here $\zeta_{j_1} = d_{j_1+1}$, $\zeta_{j_2} = d_{j_2}$ and $\zeta_j = d_j + d_{j_1+1}$ when $j_1 < j < j_2$.

Shear stress $\tau^{(n)}$ is assumed to be constant throughout the thickness of VE material based on equilibrium equation. However, since strain and temperature distribution are not uniform throughout the thickness of the VE material, therefore, the fractional derivative is written as in Eq. (8).

$$\tau^{(n)} + a_j D^{\alpha} \tau^{(n)} = G\left[\gamma_j^{(n)} + b_j D^{\alpha} \gamma_j^{(n)}\right] \tag{8}$$

where, D^{α} ($= d^{\alpha}/dt^{\alpha}$) = the fractional derivative operator, G = parameter of the fractional derivative. a_j and b_j, which show temperature sensitive, are different at each point j and these are calculated by Eq. (2). Considering the step-by-step integration scheme, Eq. (8) is expressed as follows;

$$\tau^{(n)} + \frac{a_j}{\Delta t^{\alpha}} \sum_{i=0}^{N} w^{(i)} \tau^{(n-i)} = G\left[\gamma_j^{(n)} + \frac{b_j}{\Delta t^{\alpha}} \sum_{i=0}^{N} w^{(i)} \gamma_j^{(n-i)} \right] \tag{9}$$

where, Δt = time step size, $w^{(i)}$ = weight function [1], [2], N = number of integration step.

By rearranging and manipulating about Eq. (9), strain $\gamma_j^{(n)}$ can be written by Eq. (10).

$$\gamma_j^{(n)} = \frac{\tau^{(n)}\left(\Delta t^{\alpha} + a_j w^{(0)}\right) + \tilde{A}_j - \tilde{B}_j}{G\left(\Delta t^{\alpha} + b_j w^{(0)}\right)}, \quad \tilde{A}_j = a_j \sum_{i=1}^{N} w^{(i)} \tau^{(n-i)}, \quad \tilde{B}_j = G b_j \sum_{i=1}^{N} w^{(i)} \gamma_j^{(n-i)} \tag{10a-c}$$

Then, by substituting Eq. (10a) into Eq. (7), stress $\tau^{(n)}$ is expressed by Eq. (11).

$$\tau^{(n)} = \left\{ 2G u_d^{(n)} - \sum_{j=j_1}^{j_2} \frac{\zeta_j \left(\tilde{A}_j - \tilde{B}_j\right)}{\Delta t^{\alpha} + b_j w^{(0)}} \right\} \Bigg/ \sum_{j=j_1}^{j_2} \frac{\zeta_j \left(\Delta t^{\alpha} + a_j w^{(0)}\right)}{\Delta t^{\alpha} + b_j w^{(0)}} \tag{11}$$

The damper force $F_d^{(n)}$ is calculated by Eq. (12).

$$F_d{}^{(n)} = \tau^{(n)} A_v \tag{12}$$

The temperature rise $\Delta\theta_j^{(n)}$ results form the energy dissipates for Δt at point j is expressed by Eq. (13).

$$\Delta\theta_j^{(n)} = \frac{1}{2}\left(\frac{\Delta\overline{W_j}}{s_j \rho_j} + \frac{\Delta\overline{W_{j+1}}}{s_{j+1}\rho_{j+1}} \right), \quad \Delta\overline{W_j} = \left(\tau^{(n)} + \tau^{(n-1)}\right)\left(\gamma_{j-1}^{(n)} - \gamma_{j-1}^{(n-1)} + \gamma_j^{(n)} - \gamma_j^{(n-1)}\right)/4 \tag{13a,b}$$

where $\Delta\overline{W_{j_1}} = \Delta\overline{W_{j_2+1}} = 0$ because there are steel plate parts. In order to predict the $(n+1)^{\text{th}}$ step temperature distribution of VE damper $\theta_j^{(n+1)}$, not only temperature rise form the energy dissipates $\Delta\theta_j^{(n)}$ but also temperature rise and/or fall results from the heat transfer and conduction $\overline{\theta}_j^{(n)}$ (Eq. (14)).

$$\theta_j{}^{(n+1)} = \Delta\theta_j{}^{(n)} + \overline{\theta}_j{}^{(n)}, \quad \overline{\theta}_j{}^{(n)} = \sum_{k=0}^{m} x_{jk}\ \theta_k{}^{(n)} + y_j \tag{14a,b}$$

where Eq. (14b) expresses the simplified 1D-heat transfer equation solution.

The heat-transfer coefficient, which is used in the long duration model analysis, are decided in order that the heat flow rate of the long duration model is same as 3D-FEM results. Thus, the inner plate side's heat-transfer coefficient $\alpha_{c,in}$ and the outer plate side's heat-transfer coefficient $\alpha_{c,out}$ are expressed as follows;

$$\alpha_{c,in} = Q_{in} / \{A_d (\theta_{in} - \theta_c)\}, \quad \alpha_{c,out} = Q_{out} / \{A_d (\theta_{out} - \theta_c)\} \tag{15a,b}$$

where, Q_{in} and Q_{out} = the heat flow rate at inner plate side and outer plate side obtained form 3D-FEM analysis results, respectively, θ_{in} and θ_{out} = the average temperature of surface at inner plate side and outer plate side, respectively. Then $\alpha_{c,in}$ = 0.956 N/s/cm/^{o}C, $\alpha_{c,out}$ = 0.524 N/s/cm/^{o}C.

4.2 *Comparison between Test and Long Duration Model Results*

Figure 10 shows the comparison of temperature between the test results and the analysis results which are calculated by the long duration model and by the short duration model [2]. As can be seen from Figure 10, the long duration model results agrees well with test result, however, the short duration model results fails prematurely because the short duration model can not consider the heat conduction & transfer.

Figure 11 shows damper hysteresis loop calculated by (a) the long duration model, and (b) the short duration model, respectively. Figure 12(a), (b), respectively, show the comparison of K'_d and K''_d between test and analysis results with the long duration model and the short duration model. Obviously, K'_d and K''_d calculated by the long duration model are in good agreement with the test results. However, the results which are obtained from the short duration model calculation are significantly softened due to the overestimated temperature (See Figure 10).

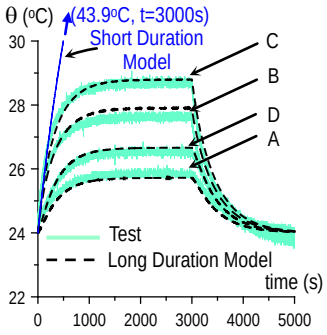

Figure10. Comparison of temperature with test and long duration model and short duration model.

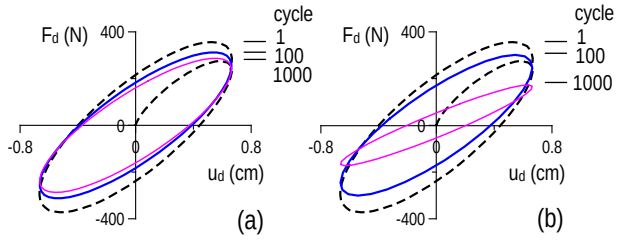

Figure 11. Comparison of loop: (a) Long duration model, (b) Short duration model

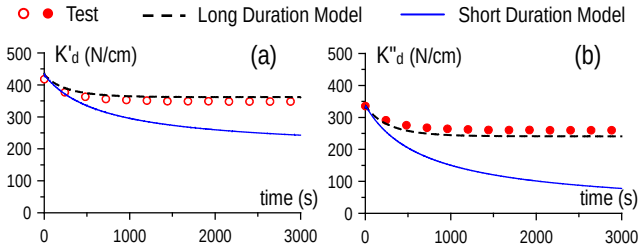

Figure 12. Comparison of K'_d , K''_d with test, long duration model and short duration model.

4.3 *Damper Properties under Long Duration Random Load and Simply Evaluation Method*

Figure 13 show the random damper deformation time history obtained from the analysis result of 1DOF model whose natural frequency f_0 = 0.33, 0.17Hz and the damping ratio ξ_0 = 2.0%. Here, (a) and (b) are the along-wind direction results, (c) and (d) are cross-direction results. These time history are normalized in order that the standard deviation σ_D = 0.467cm same as the sinusoidal-wave in Chapter 2.

Figure 14 shows the temperature time history calculated by the long duration model under the long duration random load. Analytical result shows that temperature inside the VE damper become stable by effect of heat conduction & heat transfer even if the damper is vibrating randomly.

In addition, the simplified evaluation method, which is called "sinusoidal-wave replacement method", using sinusoidal-wave which is called "replacement sinusoidal-wave" shows as follows. The replacement sinusoidal-wave's frequency f_r and amplitude A_r are expressed by Eq.

(16), respectively.

$$f_r = N_0^+ / T_a = \nu_0^+, \quad A_r = \sqrt{2}\sigma_D \qquad (16a,b)$$

where N_0^+ = number of cycle, T_a = duration time, ν_0^+ = zero crossing number.

Figure 14 shows the temperature time history calculated by the sinusoidal-wave replacement method. The results obtained from the sinusoidal-wave replacement method are excellent accuracy the results using the long random loading.

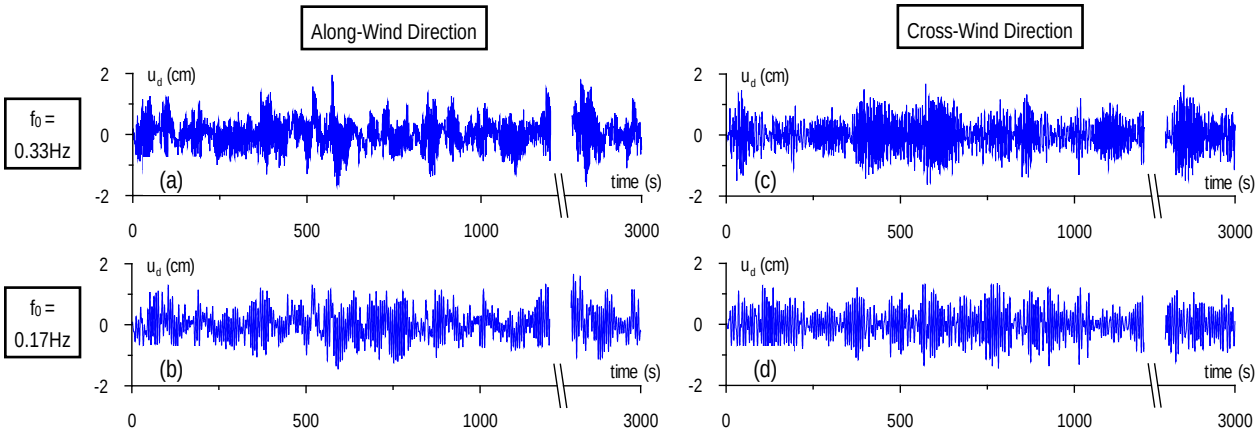

Figure 13. Time history of the damper deformation.

5 CONCLUSIONS

This paper proposed the two types of three-dimensional finite element method analysis and the one-dimensional non-linear hysteresis model of VE damper considering heat conduction and heat transfer. Good accuracy of these analysis methods are demonstrated by comparing with the test results of experiments applying cyclic loading of long duration. These models may be used for design of the VE damper and / or the building having VE damper under the long duration force such as the wind force. In addition, the simply evaluation method which can obtain the damper properties during vibrating randomly is proposed, this method gives excellent accuracy with the results using the long random loading.

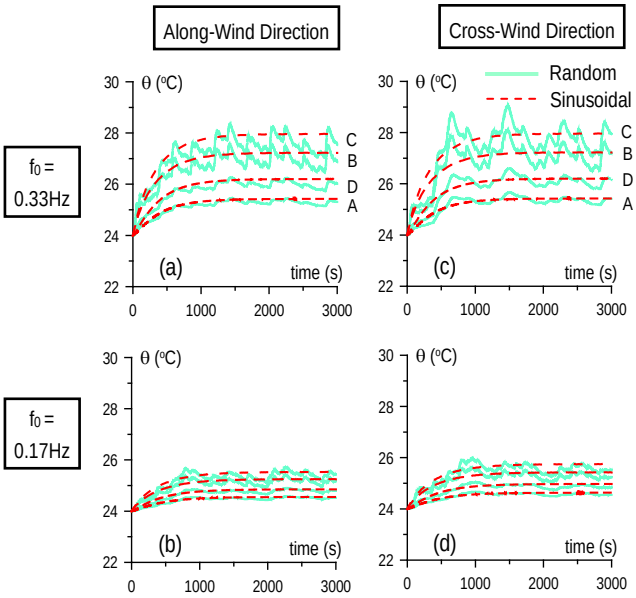

Figure 14. Comparison of temperature with random and replacement sinusoidal-wave load.

References:

[1] Kasai, K., Munshi, J.A., Lai, M.-L, and Maison, B.F., Viscoelastic Damper Hysteresis Model, Theory, Experiment, and Application ATC17-1 Seminar, Applied Technology Council, Vol1.2, 1993, pp.521-532

[2] Kasai, K., Teramoto, M., Okuma, K., and Tokoro, K., Constitutive Rule for Viscoelastic Materials Considering Temperature and Frequency Sensitivity, Journal of Structural and Construction Engineering (Transactions of AIJ), No.543, 2001. pp. 77-86, (in Japanese)

[3] J. P. Holman, Heat transfer 6th ed, McGraw-Hill, New York, 1986